Dissipation can enhance quantum effects

Joachim Ankerhold
Physikalisches Institut, Albert-Ludwigs-Universität, D-79104 Freiburg, Germany

Eli Pollak
Chemical Physics Department, Weizmann Institute of Science, 76100, Rehovoth, Israel

(Received 22 November 2006; revised manuscript received 23 January 2007; published 9 April 2007)

Usually one finds that dissipation tends to make a quantum system more classical in nature. We study the effect of momentum dissipation on a quantum system. The momentum of the particle is coupled bilinearly to the momenta of a harmonic oscillator heat bath. For a harmonic oscillator system we find that the position and momentum variances for momentum coupling are, respectively, identical to momentum and position variances for spatial friction. This implies that momentum coupling leads to an increase in the fluctuations in position as the temperature is lowered, exactly the opposite of the classical-like localization of the oscillator, found with spatial friction. For a parabolic barrier, momentum coupling causes an *increase* in the unstable normal mode barrier frequency, as compared to the lowering of the barrier frequency in the presence of purely spatial coupling. This increase in the frequency leads to an enhancement of the thermal tunneling flux, which below the crossover temperature becomes exponentially large. The crossover temperature between tunneling and thermal activation *increases* with momentum friction so that quantum effects in the escape are relevant at higher temperatures.

DOI: 10.1103/PhysRevE.75.041103 PACS number(s): 05.40.−a, 03.65.Yz, 73.40.Gk, 82.20.Xr

I. INTRODUCTION

The effect of spatial dissipation on the classical [1] and quantum [2] dynamics of a system is well understood. On a microscopic level, dissipation arises from bilinear coupling of the system coordinate to the displacement coordinates of a harmonic bath. Classically the bath modes obey forced oscillator equations of motion, which may be solved formally in terms of the motion of the system. These are then inserted in the system equation of motion which then takes the form of a generalized Langevin equation.

Over 20 years ago, Caldeira and Leggett [3] took advantage of this equivalence to study the effect of a dissipative bath on the quantum dynamics of the system, paying special attention to the quantum tunneling effect. Their central conclusion was that dissipation reduces the tunneling probability; however, it does not destroy it completely. Hence, the possibility of observing macroscopic quantum tunneling.

The detrimental effect of an interaction between the system and its environment on quantum phenomena makes intuitive sense. Consider first the localization of a particle in space. It is well known [4] that the position variance of a dissipative harmonic oscillator becomes smaller as the dissipation strength is increased. In the limit of very large Ohmic friction, the bath can localize the particle completely, without violating the uncertainty principle [5]. The bath may be thought of as creating an effective particle with a very large mass, and such a heavy particle may be localized.

One has a similar picture of how the environment destroys tunneling. For a dissipative parabolic barrier, it is well known that diagonalization of the system-bath Hamiltonian leads to an unstable mode, whose frequency decreases as the coupling strength increases [6,7]. Tunneling occurs by transmission through this collective unstable mode. Since its frequency is smaller, it is a broader barrier, the action needed to cross it increases, and the tunneling probability decreases [8]. The same qualitative picture holds at low temperatures below the crossover temperature separating the tunneling and activated barrier crossing regimes [2,3,9]. Spatial dissipation also reduces the crossover temperature [10]; it is proportional to the collective-mode barrier frequency. This lowering also fits in with the general observation that dissipation causes quantum systems to behave more like classical systems [3].

All of these conclusions are based on an extensive study of the quantum dynamics of dissipative systems, where the Hamiltonian can be brought to the form of bilinear coupling between the system and bath coordinates. There is a qualitative difference between this type of spatial dissipative coupling and bilinear momentum coupling of a system coupled to a bath [11]. Recently, Makhnovskii and Pollak [12] have shown that bilinear momentum coupling leads to stochastic acceleration [13,14] without any violation of the second law of thermodynamics [15]. In contrast to spatial coupling, which effectively increases the mass of the system, momentum coupling reduces it, and in the limit of an "Ohmic" coupling, the effective mass goes to zero. Hence, the system can undergo stochastic acceleration. This observation indicates that perhaps momentum coupling can lead to some rather anti-intuitive quantum mechanical results. If it reduces the effective mass, it should amplify quantum effects rather than destroy them. This is the topic of this paper.

In Sec. II we study the classical and quantum dynamics of a harmonic oscillator bilinearly coupled to the momentum of a harmonic bath. We find that as already noted in a different context by Cuccoli *et al.* [11], here too the effective mass is reduced such that increasing the momentum coupling increases the thermal variance of the position of the quantum particle instead of decreasing it. In Sec. III we study the dynamics of a parabolic barrier. Momentum coupling increases the thermal flux of the particle across the barrier as compared to the thermal flux in the absence of coupling. Most interestingly, the bath increases the magnitude of the

normal-mode parabolic barrier frequency, implying that it becomes thinner and therefore the tunneling flux through the barrier increases. We show that this is indeed the case both above and below the crossover temperature, which now increases with increasing coupling strength. We end in Sec. IV with a summary.

II. MOMENTUM COUPLING AND THE HARMONIC OSCILLATOR

A. Preliminaries

Our model is that of a harmonic oscillator with mass-weighted momentum P, coordinate Q, and harmonic frequency Ω interacting bilinearly with a harmonic oscillator heat bath through the momentum [12]. The Hamiltonian then takes the form

$$H = \frac{1}{2}\left[P^2 + \Omega^2 Q^2 + \sum_{j=1}^{N} (p_j - d_j P)^2 + \sum_{j=1}^{N} \omega_j^2 x_j^2 \right], \quad (1)$$

where p_j, x_j, $j=1,\ldots,N$, are the mass-weighted momentum and coordinate of the jth bath oscillator whose frequency is ω_j. The d_j's are the bilinear coupling coefficients to the particle's momentum.

Before considering the dynamics of this Hamiltonian, it is appropriate to put it into the context of previous studies of dissipative systems. The coupling of the system to the bath through the momentum of the bath has been studied previously in a variety of contexts. In an early paper, Leggett [16] considered the possibility of two coupling terms, taking the form $Q\Sigma_{j=1}^{N} d_j p_j + P\Sigma_{j=1}^{N} c_j x_j$. He then distinguishes between *normal* dissipation, where the Langevin equation of motion is derived for the spatial system coordinate Q and *anomalous* dissipation, where the Langevin equation of motion is derived for the spatial system momentum. Neither of these describe the model Hamiltonian given in Eq. (1) above. In our model, the coupling term has the form $P\Sigma_{j=1}^{N} d_j p_j$, leading to qualitatively different dynamics.

A different model has been considered by Ford *et al.* [17]. In their case the coupling to the bath takes the quadratic form $(P - \Sigma_{j=1}^{N} d_j p_j)^2$. It describes the physics of blackbody radiation in which the momentum of the particle is coupled to the magnetic field of the vacuum radiation. Such coupling also differs from that given in Eq. (1). The counterterm appearing in the model of Ford *et al.* causes a coupling between the bath modes themselves and allows one by a change of variables [17] to recast the problem into one which is equivalent in form to the standard dissipative Hamiltonian studied in detail in Refs. [3,4].

More recently, Cuccoli *et al.* [11] have studied a momentum coupling model which is identical to Eq. (1). They term this model *anomalous* dissipative coupling. However, as already discussed above, the dissipation of this model differs from the one studied by Leggett [16]. To distinguish between the two, we have used the terminology *momentum dissipation* for Eq. (1).

The formal solution of Hamilton's equations of motion for the jth bath oscillator is [12]

$$x_j(t) = x_j(0)\cos(\omega_j t) + \frac{\dot{x}_j(0)}{\omega_j}\sin(\omega_j t) - \frac{d_j}{\omega_j}\int_0^t dt' \dot{P}(t') \times \sin[\omega_j(t-t')]. \quad (2)$$

The equations of motion for the particle are

$$\dot{Q} = P - \sum_{j=1}^{N} d_j \dot{x}_j, \quad (3)$$

$$\dot{P} = -\Omega^2 Q. \quad (4)$$

Equation (4) together with

$$M\ddot{Q}(t) + \Omega^2 Q = M f_P(t) - \int_0^t dt' \dot{P}(t') M \varphi_P(t-t') \quad (5)$$

provides a generalized Langevin equation description for the motion of a particle with effective mass

$$M = \left(1 + \sum_{j=1}^{N} d_j^2\right)^{-1}. \quad (6)$$

The noise is represented by the momentum f_P random acceleration:

$$f_P(t) = \sum_{j=1}^{N} d_j \omega_j^2 \left[x_j(0)\cos(\omega_j t) + \frac{\dot{x}_j(0)}{\omega_j}\sin(\omega_j t) \right], \quad (7)$$

which has zero mean. Its correlation function is

$$\beta\langle f_P(t) f_P(0)\rangle = \sum_{j=1}^{N} d_j^2 \omega_j^2 \cos\omega_j t \equiv \eta_P(t). \quad (8)$$

The brackets denote averaging with respect to the thermal distribution ($e^{-\beta H}$). Finally, in Eq. (5) we also used the notation

$$\varphi_P(t) = \int_0^t dt'\, \eta_P(t') = \sum_{j=1}^{N} d_j^2 \omega_j \sin(\omega_j t). \quad (9)$$

The solution of the generalized Langevin equation (5) may be obtained by means of the Laplace transformation $\hat{f}(s) = \int_0^\infty dt e^{-st} f(t)$. Using the relation $\hat{\varphi}_P(s) = \hat{\eta}_P(s)/s$ one finds from Eq. (5) that the Laplace transform of the particle's coordinate is

$$\hat{Q}(s) = \frac{\dot{Q}(0) + sQ(0) + \hat{f}_P(s)}{s^2 + \Omega^2\left[\frac{1}{M} - \frac{\hat{\eta}_P(s)}{s}\right]} = \frac{\dot{Q}(0) + sQ(0) + \hat{f}_P(s)}{s^2\left(1 + \Omega^2 \sum_{j=1}^{N} \frac{d_j^2}{s^2 + \omega_j^2}\right)}. \quad (10)$$

Noting that

$$\langle \dot{Q}^2 \rangle = \frac{\langle P^2 \rangle}{M} = \frac{1}{\beta M}, \quad (11)$$

one readily finds that the classical velocity correlation function is

$$\langle \dot{Q}(t)\dot{Q}(0)\rangle = \text{i.l.t.}\left(\frac{s}{\beta} \cdot \frac{\frac{1}{M} - \frac{\hat{\eta}(s)}{s}}{s^2 + \Omega^2\left[\frac{1}{M} - \frac{\hat{\eta}_P(s)}{s}\right]} \right), \quad (12)$$

where i.l.t. stands for "inverse Laplace transform."

To express results in the continuum limit it is useful to define a momentum spectral density as

$$J_P(\omega) = \frac{\pi}{2}\sum_{j=1}^{N} d_j^2 \omega_j^3 \delta(\omega - \omega_j), \quad (13)$$

where $\delta(x)$ is the Dirac delta-function. As a result, the momentum function $\eta_P(t)$ may be expressed in terms of the spectral density as

$$\eta_P(t) = \frac{2}{\pi}\int_0^\infty d\omega \frac{J_P(\omega)}{\omega}\cos(\omega t). \quad (14)$$

B. Normal-mode transformation

Additional insight as well as solution of the associated quantum dynamics is facilitated by considering the normal-mode representation. The Hamiltonian given in Eq. (1) has a quadratic form and so may be diagonalized. For this purpose we define frequency-weighted coordinates and momenta as

$$\bar{Q} = \Omega Q, \quad \bar{P} = P/\Omega, \quad (15)$$

$$\bar{x}_j = \omega_j x_j, \quad \bar{p}_j = p_j/\omega_j, \quad j = 1, \ldots, N, \quad (16)$$

so that the coordinate part of the Hamiltonian has unit frequency:

$$H = \frac{1}{2}\left[\Omega^2 \bar{P}^2 + \sum_{j=1}^{N} \omega_j^2 \left(\bar{p}_j - \frac{d_j}{\omega_j}\Omega \bar{P} \right)^2 + \bar{Q}^2 + \sum_{j=1}^{N} \bar{x}_j^2 \right]. \quad (17)$$

The $N+1$ normal modes and associated momenta are denoted as y_j, p_{yj}, $j=0,\ldots,N$, such that the normal-mode form of the Hamiltonian is

$$H = \frac{1}{2}\sum_{j=0}^{N} (\lambda_j^2 p_{y_j}^2 + y_j^2) \quad (18)$$

and the λ_j's are the normal-mode frequencies. This transformation implies that the vector of normal-mode momenta $\mathbf{p}_y$ is an orthogonal transformation of the frequency-weighted momenta such that

$$\mathbf{p}_y = \mathbf{U}\begin{pmatrix} \bar{P} \\ \bar{\mathbf{p}} \end{pmatrix}, \quad (19)$$

where $\mathbf{U}$ is an $(N+1)\times(N+1)$ orthogonal transformation matrix.

Following the same considerations as in the Appendix of Ref. [18] one readily finds that the normal-mode frequencies are the $N+1$ solutions of the equation

$$\lambda_k^2 = \frac{\Omega^2}{1 + \Omega^2 \sum_{j=1}^{N} \frac{d_j^2}{\omega_j^2 - \lambda_k^2}}. \quad (20)$$

The elements of the transformation matrix are then given by

$$u_{kj} = \frac{d_j \omega_j \Omega}{\omega_j^2 - \lambda_k^2} u_{k0}, \quad j = 1, \ldots, N, \quad k = 0, \ldots, N, \quad (21)$$

$$u_{k0}^2 = \left(1 + \Omega^2 \sum_{j=1}^{N} \frac{d_j^2 \omega_j^2}{(\omega_j^2 - \lambda_k^2)^2} \right)^{-1}, \quad k = 0, \ldots, N. \quad (22)$$

By considering the 00 element of the $(N+1)\times(N+1)$ matrix $(\mathbf{T}'' + s^2\mathbf{I})^{-1}$ (where $\mathbf{T}''$ is the matrix of second derivatives of the kinetic energy of the Hamiltonian with respect to the frequency scaled momenta) one finds the important identity

$$\sum_{j=0}^{N} \frac{u_{j0}^2}{s^2 + \lambda_j^2} = \left[s^2 + \Omega^2 \left(\frac{1}{M} - \frac{\hat{\eta}_P(s)}{s} \right) \right]^{-1}. \quad (23)$$

This identity then leads directly to all classical results of interest in the continuum limit [19].

For this purpose we also define a normal-mode momentum function as

$$K(t) = \sum_{j=0}^{N} u_{j0}^2 \cos(\lambda_j t). \quad (24)$$

A spectral density of the normal modes is then defined as [20]

$$\Upsilon(\lambda) = \frac{\pi}{2}\sum_{j=0}^{N} u_{j0}^2 \lambda_j [\delta(\lambda - \lambda_j) - \delta(\lambda + \lambda_j)]. \quad (25)$$

One now notes that the Laplace transform of the normal-mode momentum function may be expressed directly in terms of the original momentum function:

$$\frac{\hat{K}(s)}{s} = \sum_{j=0}^{N} \frac{u_{j0}^2}{s^2 + \lambda_j^2} = \left[s^2 + \Omega^2 \left(\frac{1}{M} - \frac{\hat{\eta}_P(s)}{s} \right) \right]^{-1}. \quad (26)$$

Using the Fourier decomposition of the Dirac δ function $[\pi\delta(\lambda) = \int_0^\infty dt \cos(\lambda t)]$ we find that the spectral density of the normal modes may also be expressed in the continuum limit as

$$\Upsilon(\lambda) = \text{Re}[\lambda \hat{K}(i\lambda)]. \quad (27)$$

We further note that at equilibrium,

$$\langle y_j^2 \rangle = k_B T, \quad j = 0, \ldots, N, \quad (28)$$

$$\langle \dot{y}_j^2 \rangle = \lambda_j^4 \langle p_{y_j}^2 \rangle = \lambda_j^2 k_B T, \quad j = 0, \ldots, N. \quad (29)$$

With these preliminaries it becomes straightforward to solve for thermal correlation functions. Since the Hamiltonian is diagonal in the normal modes, one has trivially that the solution of the jth normal mode is

$$y_j(t) = y_j(0)\cos(\lambda_j t) + \frac{\dot{y}_j(0)}{\lambda_j}\sin(\lambda_j t), \quad j = 0, \ldots, N. \tag{30}$$

The system coordinate is just a linear combination of the normal modes,

$$Q(t) = \frac{\bar{Q}(t)}{\Omega} = \frac{\sum_{j=0}^{N} u_{j0} y_j(t)}{\Omega}, \tag{31}$$

so that

$$\langle Q(t)Q(0)\rangle = \frac{\sum_{j=0}^{N} u_{j0}^2 \langle y_j^2\rangle \cos(\lambda_j t)}{\Omega^2} = \frac{K(t)}{\beta\Omega^2}. \tag{32}$$

Similarly

$$\langle \dot{Q}(t)\dot{Q}(0)\rangle = -\frac{\ddot{K}(t)}{\beta\Omega^2}. \tag{33}$$

These properties of the normal-mode transformation become very useful also when considering the barrier crossing dynamics, as described in Sec. III, below.

C. Quantum dynamics

In the quantum regime one may work with the normal modes and use the quantum instead of the classical expressions (28) and (29). For the equilibrium variances the procedure is then as follows. From the quantum mechanical expressions

$$\langle y_j^2\rangle = \frac{\hbar\lambda_j}{2}\coth\left(\frac{\hbar\beta\lambda_j}{2}\right), \tag{34}$$

it follows that

$$\langle Q^2\rangle = \frac{\hbar}{2\Omega^2}\sum_{j=0}^{N} u_{j0}^2 \lambda_j \coth\left(\frac{\hbar\beta\lambda_j}{2}\right). \tag{35}$$

Using the decomposition [21]

$$\coth(\pi x) = \frac{1}{\pi x} + \frac{2x}{\pi}\sum_{k=1}^{\infty}\frac{1}{x^2 + k^2}, \tag{36}$$

we arrive at

$$\langle Q^2\rangle = \frac{1}{\beta\Omega^2}\left[1 + 2\sum_{j=0}^{N} u_{j0}^2 \lambda_j^2 \sum_{k=1}^{\infty}\frac{1}{\lambda_j^2 + \nu_k^2}\right], \tag{37}$$

with the Matsubara frequencies $\nu_k = 2\pi k/(\hbar\beta)$. Interchanging the sums, using the fact $\Sigma_{j=0}^{N} u_{j0}^2 = 1$, and using the identity (23) gives us

$$\langle Q^2\rangle = \frac{1}{\beta\Omega^2}\left[1 + 2\sum_{k=1}^{\infty}\left(\frac{\Omega^2\left(\frac{1}{M} - \frac{\hat{\eta}_P(\nu_k)}{\nu_k}\right)}{\nu_k^2 + \Omega^2\left(\frac{1}{M} - \frac{\hat{\eta}_P(\nu_k)}{\nu_k}\right)}\right)\right]. \tag{38}$$

It is worthwhile to derive a similar expression for the momentum. In this case,

$$\langle P^2\rangle = \Omega^2\sum_{j=0}^{N} u_{j0}^2 \langle p_{y_j}^2\rangle, \tag{39}$$

with $\langle p_{y_j}^2\rangle = (\hbar/2\lambda_j)\coth(\hbar\beta\lambda_j/2)$. It follows that

$$\begin{aligned}\langle P^2\rangle &= \frac{\hbar}{2}\Omega^2\sum_{j=0}^{N}\frac{u_{j0}^2}{\lambda_j}\coth\left(\frac{\hbar\beta\lambda_j}{2}\right) \\ &= \frac{1}{\beta}\left[1 + 2\Omega^2\sum_{j=0}^{N}\sum_{k=1}^{\infty}\frac{u_{j0}^2}{\lambda_j^2 + \nu_k^2}\right],\end{aligned} \tag{40}$$

where we used the identity [obtained from Eq. (23) in the limit that $s \to 0$] that

$$\sum_{j=0}^{N}\frac{u_{j0}^2}{\lambda_j^2} = \frac{1}{\Omega^2}. \tag{41}$$

Finally using again the identity (23) one obtains

$$\langle P^2\rangle = \frac{1}{\beta}\left[1 + 2\Omega^2\sum_{k=1}^{\infty}\frac{1}{\nu_k^2 + \Omega^2\left(\frac{1}{M} - \frac{\hat{\eta}_P(\nu_k)}{\nu_k}\right)}\right]. \tag{42}$$

It is instructive to derive the quantum mechanical correlations along an alternative route, which for spatial friction has been discussed in Refs. [2,19] and only exploits fundamental principles of quantum statistical mechanics. Namely, since the equations of motion for the Heisenberg operators $Q(t)$ and $P(t)$ are linear, the following is true: (i) Due to Ehrenfest's theorem, the quantum mechanical averages obey classical equations of motion, (ii) correlation functions can be obtained from the quantum version of the fluctuation dissipation theorem, and (iii) mean values and second-order correlations completely determine the quantum dynamics since all random forces are related to a stationary Gaussian process.

When using (ii) one has to take into account that according to Eq. (3) and in contrast to spatial friction the time derivative of Q is not identical to P. Hence, to apply the fluctuation dissipation theorem we do not start from the equation of motion in position (5), but from the corresponding expression in momentum, i.e.,

$$\langle \ddot{P}(t)\rangle + \frac{\Omega^2}{M}\langle P(t)\rangle - \Omega^2\int_0^t dt'\langle P(t')\rangle\varphi_P(t-t') = 0, \tag{43}$$

and calculate according to (i) the classical response

$$\langle P(t)\rangle = \int_0^t dt' \chi_P(t-t')F(t') \tag{44}$$

to an external force $F(t)$ applied for $t>0$. In Fourier space the above equation reads $\langle \tilde{P}(\omega)\rangle = \tilde{\chi}_P(\omega)\tilde{F}(\omega)$ so that

$$\tilde{\chi}_P(\omega) = \frac{\Omega^2}{\Omega^2/M - \omega^2 - \Omega^2\tilde{\varphi}_P(\omega)}, \tag{45}$$

with $\tilde{\varphi}_P(\omega) = \hat{\eta}_P(-i\omega)/(-i\omega)$.

According to (ii) it is now the symmetrized momentum correlation $S_P(t) = (1/2)\langle P(t)P(0) + P(0)P(t)\rangle$, which is related to the imaginary part of the response function $\tilde{\chi}_P = \tilde{\chi}'_P + i\tilde{\chi}''_P$ via

$$\tilde{S}_P(\omega) = \hbar \coth(\omega\hbar\beta/2)\tilde{\chi}''_P(\omega). \tag{46}$$

Further, due to Eq. (44), the antisymmetrized momentum correlation function $A_P(t) = (1/i)[P(t), P(0)]$ is related to the response function via

$$\chi_P(t) = -\frac{2}{\hbar}\theta(t)A_P(t), \tag{47}$$

with the step function $\theta(\cdot)$. Thus, in the time domain we arrive at the general expressions

$$S_P(t) = \frac{\hbar}{2\pi}\int_{-\infty}^{\infty} d\omega \tilde{\chi}''_P(\omega)\coth(\omega\hbar\beta/2)\cos(\omega t) \tag{48}$$

and

$$A_P(t) = -\frac{\hbar}{2\pi}\int_{-\infty}^{\infty} d\omega \tilde{\chi}''_P(\omega)\sin(\omega t), \tag{49}$$

from which following (iii) all real-time correlations can be derived—e.g., $\langle Q(t)Q(0)\rangle = \langle \dot{P}(t)\dot{P}(0)\rangle/\Omega^4 = [-\ddot{S}_P(t) - i\ddot{A}_P(t)]/\Omega^4$. For analytical calculations it is sometimes more convenient to work with representations based on Laplace transforms: namely,

$$\hat{A}_P(s) = -\frac{\hbar}{2}\hat{\chi}_P(s),$$

$$\hat{S}_P(s) = \frac{1}{\beta}\sum_{n=-\infty}^{\infty} \frac{s}{\nu_n^2 - s^2}[\hat{\chi}_P(s) - \hat{\chi}_P(|\nu_n|)], \tag{50}$$

where we used that $\hat{\chi}_P(s) = \tilde{\chi}_P(is)$.

By considering $S_P(0) = -\lim_{s\to\infty} s\hat{S}_P(s)$ one obtains the equilibrium variance in momentum

$$\langle P^2\rangle_\beta = \frac{1}{\beta}\sum_{n=-\infty}^{\infty}\hat{\chi}_P(|\nu_n|) = \frac{1}{\beta} + \frac{2\Omega^2}{\beta}\sum_{n=1}^{\infty}\frac{1}{\Omega^2\left(\frac{1}{M} - \frac{\hat{\eta}(\nu_n)}{\nu_n}\right) + \nu_n^2}. \tag{51}$$

which is, of course, identical to Eq. (42). For the position $\langle Q^2\rangle_\beta = -\ddot{S}_P(0)/\Omega^4$ one must be careful when taking the limit in $\ddot{S}_P(0) = \lim_{s\to\infty} s^3\hat{S}_P(s)$ due to singularities which must be properly subtracted. One gets

$$\langle Q^2\rangle_\beta = \frac{2}{\beta\Omega^4}\sum_{n=-\infty}^{\infty}[\Omega^2 - \nu_n^2\hat{\chi}_P(|\nu_n|)]$$

$$= \frac{1}{\Omega^2\beta} + \frac{2}{\beta}\sum_{n=1}^{\infty}\frac{\frac{1}{M} - \frac{\hat{\eta}_P(\nu_n)}{\nu_n}}{\nu_n^2 + \Omega^2\left[\frac{1}{M} - \frac{\hat{\eta}_P(\nu_n)}{\nu_n}\right]}, \tag{52}$$

which is identical to Eq. (38). When comparing the above expressions with those derived for spatial friction [2,19], one observes that they can be related to each other by $\Omega Q \leftrightarrow P$, which, of course, is a direct consequence of the symmetry of the Hamiltonian (1). This means, though, that all findings known for spatial friction and, e.g., Ohmic damping can be directly translated to momentum friction. We will discuss explicit results in the next section.

D. An example

To obtain a feeling for the various results presented in this section it is worthwhile to consider the specific case of a momentum density with a cutoff:

$$J_P(\omega) = \frac{\pi}{2}\gamma\omega^3\theta(\omega_c - \omega), \tag{53}$$

where $\theta(x)$ is the Heaviside function. One then finds that the Laplace transform of the momentum function is

$$\hat{\eta}_P(s) = \gamma s\left[\omega_c - s\arctan\left(\frac{\omega_c}{s}\right)\right]$$

and the mass factor

$$M = (1 + \gamma\omega_c)^{-1},$$

explicitly demonstrating that in the limit that the cutoff frequency goes to infinity, the effective mass goes to zero.

Now, let us first look at the friction dependence of the Laplace transform $\hat{\chi}_P(s)$ which directly provides the momentum variance and the functions $A_P(t)$ and $S_P(t)$. From

$$\frac{1}{M} - \frac{\hat{\eta}_P(s)}{s} = 1 + \gamma s\arctan(\omega_c/s), \tag{54}$$

we see that in the limit $\omega_c \to 0$ the friction term in $\hat{\chi}_P$ combines with the potential term to yield the effective frequency $\Omega_{\text{eff}} = \Omega\sqrt{1+\gamma\omega_c}$ of an undamped harmonic oscillator. The corresponding variance $\langle P^2\rangle$ as well as $A_P(t)$ and $S_P(t)$ is thus trivial. In the opposite limit of very large $\omega_c \gg \Omega, \gamma\Omega^2$ one has in $\hat{\chi}_P$ the expression $s^2 + \Omega^2 + \Omega^2\gamma\pi s/2$, which coincides with the form of the response function for spatial friction in the Ohmic case (friction constant γ_s) with the translation $\gamma_s = \Omega^2\gamma\pi/2$. Thus, the corresponding results can be read off from the literature [2,4]. In particular, for large cutoff and $\gamma\Omega^2\pi/2 \geqslant 1$ the time-dependent correlations decay to zero monotonously, while for $\gamma\Omega^2\pi/2 < 1$ they decay via damped oscillations. In contrast to $A_P(t)$ which displays only classical

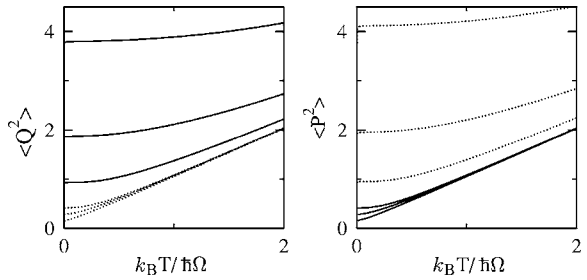

FIG. 1. Position variances (left, scaled with $\hbar/\Omega$) and momentum variances (right, scaled with $\hbar\Omega$) for momentum friction (solid lines) and for the corresponding spatial case (dotted lines) for various values of the friction strength $\gamma\Omega=0.5,2,7$: left, solid from bottom to top; left dotted from top to bottom; right, solid from top to bottom; right, dotted from bottom to top. The cutoff frequency is $\omega_c/\Omega=10$. For the spatial case a model with Drude damping (cutoff ω_c) is used with equivalent friction strength $\gamma_s=\gamma\Omega^2\pi/2$.

dynamics, $S_P(t)$ contains an additional contribution depending on the Matsubara frequencies that becomes relevant at lower temperatures. In the limit of zero temperature $S_P(t)$ then decays in time no longer exponentially but algebraically $\propto 1/t^2$. Further in the limit of zero temperature one has for the momentum variance

$$\langle P^2\rangle_0 \approx \frac{2\hbar}{\gamma\pi^2}\ln\left(\frac{\Omega^2\gamma^2\pi^2}{2}\right). \tag{55}$$

In essence, momentum friction gives for momentum correlations the same results as spatial coupling for position correlations. The same is true when the ratios ω_c/Ω, $\omega_c/\gamma\Omega^2$ decrease, but are still large, and one compares momentum friction with γ,ω_c with the well-known Drude model for spatial friction, $J_D=\gamma_s\omega\exp(-\omega/\omega_c)$, with $\gamma_s=\gamma\Omega^2\pi/2$.

Let us now turn to $\langle Q^2\rangle$, for which the limit $\omega_c\to\infty$ cannot be taken. We gain

$$\langle Q^2\rangle = \langle P^2\rangle/\Omega^2 + \frac{2\Omega^4\gamma}{\beta}\sum_{n=1}^{\infty}\frac{\nu_n \arctan(\omega_c/\nu_n)}{\nu_n^2+\Omega^2+\Omega^2\gamma\nu_n\arctan(\omega_c/\nu_n)}, \tag{56}$$

which for zero temperature, where the sum over Matsubara frequencies must be replaced by integrals according to $(2/\hbar\beta)\Sigma f(\nu_n)\to(1/\pi)\int d\nu f(\nu)$, reads for strong friction (but still $\omega_c \gg \gamma\Omega^2$)

$$\langle Q^2\rangle_0 \approx \frac{\hbar\Omega^4\gamma}{2}\ln\left(\frac{2\omega_c}{\pi\gamma\Omega^2}\right). \tag{57}$$

When dealing with spatial friction, the momentum variance for a Drude model with $\gamma_s=\gamma\Omega^2\pi/2$ is given by $\langle P^2\rangle_{\text{spatial}} \approx (\hbar\Omega^2\gamma/2)\ln(\omega_c/\Omega)$ [2]. One thus notes that the roles of the momentum and position variances are interchanged when considering the momentum coupling model. In Fig. 1 the position and momentum variances are shown for momentum coupling with the spectral density (53) together with spatial coupling with a Drude spectral density, $J_D=\gamma_s\omega\exp(-\omega/\omega_c)$. Note that the latter one is, apart from its widespread use, a sort of minimal model for spatial friction leading to well-behaved variances. In the case of momentum coupling the spectral density (53) plays a similar role. Both models give identical results for sufficiently large cutoff and $\gamma_s=\Omega^2\gamma\pi/2$—i.e., $\Omega^2\langle P^2\rangle_{\text{momentum}}(\gamma)=\langle Q^2\rangle_{\text{spatial}}(\Omega^2\gamma\pi/2)$. They differ though in the low-temperature range for the variances $\langle Q^2\rangle_{\text{momentum}}$ and $\langle P^2\rangle_{\text{spatial}}$, which are only well behaved for a finite cutoff. Of course, when for spatial friction a spectral density is taken that produces the same damping dependence in the response function as the one given by Eq. (53), we would obtain fully identical results. Accordingly, position variances are enhanced for momentum coupling and suppressed for spatial coupling and vice versa for the momentum variances. One also observes that at low temperatures the momentum variance for momentum friction is suppressed compared to the position variance for spatial friction within a Drude model [see (57)]. Accordingly, the uncertainty product for $T=0$,

$$\langle Q^2\rangle_0\langle P^2\rangle_0 = \frac{\hbar^2}{\pi^2}\ln\left(\frac{2\omega_c}{\pi\gamma\Omega^2}\right)\ln\left(\frac{\pi^2\gamma^2\Omega^2}{2}\right), \tag{58}$$

is smaller compared to the spatial case (Drude damping) by the factor $[1-\ln(\pi\gamma\Omega/2)/\ln(\omega_c/\Omega)]$.

III. CLASSICAL AND QUANTUM RATE THEORY

A. Classical rate theory in the presence of momentum coupling

We first consider the case of a parabolic barrier Hamiltonian

$$H=\frac{1}{2}\left[P^2-\Omega^{\ddagger 2}Q^2+\sum_{j=1}^{N}(p_j-d_jP)^2+\sum_{j=1}^{N}\omega_j^2x_j^2\right]. \tag{59}$$

In conventional transition-state theory (TST) one uses the system coordinate as the reaction coordinate and the dividing surface is taken to be perpendicular to it. The thermal unidirectional flux through the dividing surface is [22,23]

$$F_{TST}=\int_{-\infty}^{\infty}dPdQ\prod_{j=1}^{N}dp_jdx_je^{-\beta H}\delta(Q)\dot{Q}\theta(\dot{Q}) = \frac{1}{\beta\sqrt{M}}\prod_{j=1}^{N}\left(\frac{2\pi}{\beta\omega_j}\right). \tag{60}$$

It is noteworthy that the thermal flux through the dividing surface is larger by the factor $1/\sqrt{M}$ as compared to the conventional TST flux in the presence of only spatial coupling to the harmonic bath ($F_0=\sqrt{M}F_{TST}$). Momentum coupling causes an *enhancement* of the reaction rate.

The minimal unidirectional thermal flux is obtained by transforming the Hamiltonian to normal modes. Due to the negative force constant associated with the barrier, one will

now find after diagonalization N stable modes with frequencies λ_j and one unstable mode with barrier frequency $\lambda^{\ddagger}$. The variational TST (VTST) flux is obtained by considering the flux perpendicular to the unstable mode, and one finds that

$$F_{VTST} = \frac{1}{\beta}\prod_{j=1}^{N}\left(\frac{2\pi}{\beta\lambda_j}\right). \tag{61}$$

By considering the determinant of the second derivative matrix of the kinetic energy in the normal-mode representation and in the original coordinates one readily finds the identity

$$\lambda^{\ddagger 2}\prod_{j=1}^{N}\lambda_j^2 = \Omega^{\ddagger 2}\prod_{j=1}^{N}\omega_j^2. \tag{62}$$

As a result the ratio of the VTST flux to the TST flux is

$$\frac{F_{VTST}}{F_{TST}} = \sqrt{M}\frac{\lambda^{\ddagger}}{\Omega^{\ddagger}}. \tag{63}$$

The analog of the Kramers-Grote-Hynes equation [24,25] for the normal-mode barrier frequency in the presence of spatial diffusion is obtained from Eq. (20), except that one substitutes the stable-mode frequency with the unstable-mode frequency. After a bit of rearranging one finds

$$\lambda^{\ddagger 2} + \frac{\Omega^{\ddagger 2}\hat{\eta}_P(\lambda^{\ddagger})}{\lambda^{\ddagger}} = \frac{\Omega^{\ddagger 2}}{M}, \tag{64}$$

from which it follows that $\sqrt{M}\frac{\lambda^{\ddagger}}{\Omega^{\ddagger}} \leqslant 1$ and as expected the VTST flux is lower than the TST flux. Note, however, that Eq. (64) may also be rewritten as

$$\frac{\lambda^{\ddagger 2}}{\Omega^{\ddagger 2}} = 1 + \lambda^{\ddagger 2}\sum_{j=1}^{N}\frac{d_j^2}{\omega_j^2 + \lambda^{\ddagger 2}}, \tag{65}$$

showing that momentum coupling leads to a *thinning* of the barrier, instead of the usual broadening of the barrier found as a result of spatial coupling. In fact, the ratio $\frac{F_{VTST}}{F_0} = \frac{\lambda^{\ddagger}}{\Omega^{\ddagger}}$, implying that even the minimal VTST flux is *larger* then the flux in the absence of coupling. This is proof that, classically, momentum coupling leads to an increase of the thermal parabolic barrier crossing rate, as compared with the absence of coupling.

It is instructive to consider a specific example: namely, the spectral density given in Eq. (53). Using the reduced values $x = \lambda^{\ddagger}/\Omega^{\ddagger}$, $w_c = \omega_c/\Omega^{\ddagger}$, and $g = \gamma\Omega^{\ddagger}$ we plot in Fig. 2 the reduced barrier height as a function of the reduced momentum coupling coefficient g for three representative values of the reduced cutoff frequency w_c. As noted from the figure, only when the cutoff frequency is large does one get an appreciable increase in the barrier frequency. In the limit of $g \gg w_c$ one has that $x \sim \sqrt{g w_c}$. In Fig. 3 we then plot the ratio F_{VTST}/F_{TST} for the same parameter range as in Fig. 2. One notes that there is an appreciable effect on the transmission factor only when the cutoff frequency is much larger than unity. In contrast to the spatial coupling case, here the transmission factor tends to unity both in the weak- and strong-momentum-coupling limits.

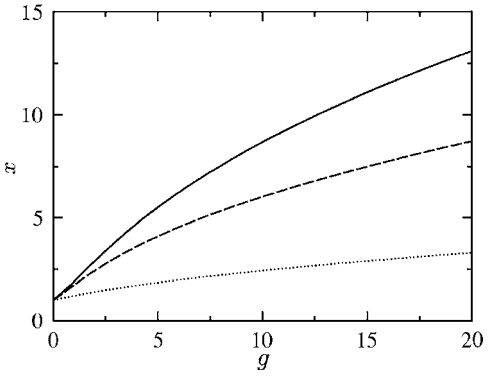

FIG. 2. Classical enhancement of the reactive flux as a result of momentum coupling to a harmonic bath: The parabolic barrier frequency is plotted as a function of the coupling strength for three different values of the cutoff frequency. The reduced barrier frequency is also the ratio of the exact thermal unidirectional flux to the flux in the absence of coupling to the bath. The solid line is for $w_c = 10$, the dashed line is for $w_c = 4$, and the dotted line is for $w_c = 0.5$.

B. Quantum rate theory in the presence of momentum coupling

Given the fact that momentum coupling causes a decrease in the barrier width, it is interesting to study whether it could then cause an increase in the tunneling probability, since the tunneling probability is exponentially sensitive to the width of the barrier. We will consider two cases. The first is transmission through a parabolic barrier. The second will be consideration of tunneling through an anharmonic barrier in the limit of weak momentum coupling and at temperatures which are below the crossover temperature between tunneling and thermal activation. We will see that the two limits give qualitatively identical results. Above the crossover temperature, where the parabolic barrier approximation is valid, we find that momentum coupling indeed causes an increase

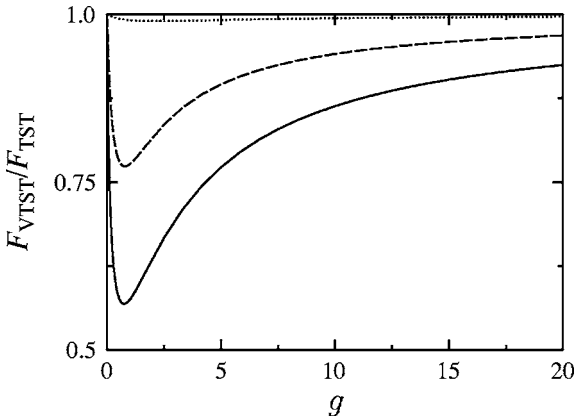

FIG. 3. VTST solution for the classical transmission factor through a parabolic barrier potential as compared to choosing the system coordinate as the reaction coordinate. The three lines correspond to the same values of the cutoff frequency as in Fig. 2.

of the rate which is even greater than the classical enhancement. This is due to the thinning of the parabolic barrier. At low temperatures, below the crossover temperature, momentum coupling leads even to an exponential increase in the tunneling rate.

1. Above the crossover temperature

In the limit of a parabolic barrier, we follow the same reasoning as for spatial diffusion, as given in Ref. [6]. In the absence of momentum coupling, the thermal fraction through the barrier is

$$F_0^Q = 2^{-N}\frac{\hbar\Omega^\ddagger}{2}\sin\left(\frac{\hbar\beta\Omega^\ddagger}{2}\right)^{-1}\prod_{j=1}^{N}\sinh\left(\frac{\hbar\beta\omega_j}{2}\right)^{-1}, \quad (66)$$

while the VTST tunneling fraction is given by the same expression, except one must replace the bare frequencies everywhere with the normal-mode frequencies. One thus has that the quantum transmission factor is

$$\frac{F_{VTST}^Q}{F_0^Q} = \frac{\lambda^\ddagger}{\Omega^\ddagger}\frac{\sin\left(\frac{\hbar\beta\Omega^\ddagger}{2}\right)}{\sin\left(\frac{\hbar\beta\lambda^\ddagger}{2}\right)}\prod_{j=1}^{N}\frac{\sinh\left(\frac{\hbar\beta\omega_j}{2}\right)}{\sinh\left(\frac{\hbar\beta\lambda_j}{2}\right)}. \quad (67)$$

However, we know that the barrier frequency $\lambda^\ddagger \geqslant \Omega^\ddagger$. The denominator with the sine function will diverge at the temperature $\hbar\beta_c\lambda^\ddagger = 2\pi$; that is, the crossover temperature will be *greater* than the crossover temperature in the absence of coupling. In contrast to spatial coupling, which reduces the crossover temperature, momentum coupling increases it. At the crossover temperature, the quantum transmission factor will diverge, implying that the quantum transmission factor is indeed *larger* than the classical one. As noted, for the parabolic barrier, momentum coupling enhances tunneling.

The result for the tunneling fraction has to be transformed so that it may be expressed in the continuum limit. For this purpose one uses the infinite product representation of the sine and sinh functions (as detailed in Ref. [26]) as well as the identity

$$\det(\mathbf{T}'' + s^2\mathbf{I}) = (-\lambda^{\ddagger 2} + s^2)\prod_{j=1}^{N}(\lambda_j^2 + s^2)$$
$$= \left(-\frac{\Omega^{\ddagger 2}}{M} + s^2 + \Omega^{\ddagger 2}\frac{\hat{\eta}_P(s)}{s}\right)\prod_{j=1}^{N}(\omega_j^2 + s^2), \quad (68)$$

where as before $\mathbf{T}''$ represents the matrix of second derivatives of the kinetic energy with respect to the (frequency scaled) momenta. The last equality on the right-hand side is obtained by carrying out explicitly the evaluation of the determinant, using the frequency-scaled momenta, as given in Eqs. (15) and (16). One then finally finds that

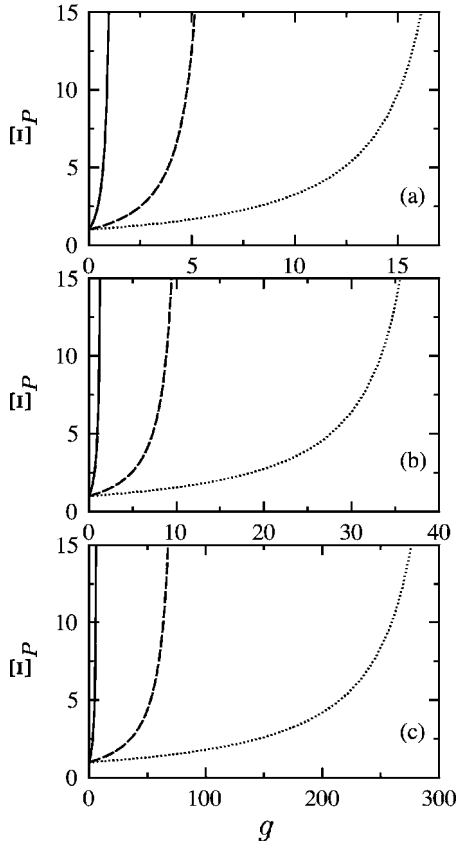

FIG. 4. Macroscopic enhancement of the quantum tunneling rate above crossover due to momentum coupling to a harmonic bath. Panels (a), (b), and (c) correspond to the cutoff frequencies 10, 4, and 0.5, respectively. In each panel we plot the dependence of the Wolynes enhancement factor as a function of the coupling strength for three different temperature values. Defining $\theta = \hbar\beta\Omega^\ddagger$, the dotted, dashed, and solid lines correspond to $\theta = 0.5$, 1, and 3, respectively. Note the change in scale for the coupling strength as one goes from panel (a) to panel (c). For low cutoff frequencies, the enhancement is weakened.

$$\frac{F_{VTST}^Q}{F_0^Q} = \frac{\lambda^\ddagger}{\Omega^\ddagger}\prod_{k=1}^{\infty}\frac{\nu_k^2 - \Omega^{\ddagger 2}}{\nu_k^2 - \frac{\Omega^{\ddagger 2}}{M} + \Omega^{\ddagger 2}\frac{\hat{\eta}_P(\nu_k)}{\nu_k}} \equiv \frac{\lambda^\ddagger}{\Omega^\ddagger}\Xi_P, \quad (69)$$

where $\nu_k = \frac{2k\pi}{\hbar\beta}$ are the Matsubara frequencies and Ξ_P is the Wolynes factor [27] associated with momentum coupling.

For the specific spectral density given in Eq. (53) one finds that the Wolynes factor is

$$\Xi_P = \prod_{k=1}^{\infty}\frac{\nu_k^2 - \Omega^{\ddagger 2}}{\nu_k^2 - \Omega^{\ddagger 2}\left[1 + \gamma\nu_k\arctan\left(\frac{\omega_c}{\nu_k}\right)\right]}, \quad (70)$$

showing clearly that the quantum enhancement of the rate due to momentum coupling is *greater* than the classical enhancement, since in the classical limit the Wolynes factor tends to unity. In Fig. 4 we plot this Wolynes factor as a function of the reduced momentum coupling coefficient $g = \gamma\Omega$ and reduced cutoff frequency $w_c = \omega_c/\Omega$.

2. Tunneling through an anharmonic barrier below the crossover temperature

For tunneling through an anharmonic barrier potential $V(Q)$ with a barrier top located at $Q=Q_b$ the escape rate Γ is most conveniently calculated from the imaginary part of the free energy and thus from the imaginary part of the partition function of the unstable system [2,3]. In the path integral representation one has for the reduced system

$$Z = \mathrm{Tr}\{e^{-\beta H}\} = \oint \mathcal{D}[Q] e^{-S_{\mathrm{eff}}[Q]/\hbar}, \tag{71}$$

where one sums over all periodic paths running in the imaginary time interval $\hbar\beta$ through the inverted barrier potential $-V(q)$. Here for momentum friction the effective action is found to read

$$S_{\mathrm{eff}}[Q] = \int_0^{\hbar\beta} d\tau \left\{ \frac{1}{2}\dot{Q}(\tau)^2 + V(Q) + \frac{1}{2}\int_0^{\hbar\beta} d\sigma \dot{Q}(\tau) \times \tilde{M}(\tau-\sigma)\dot{Q}(\sigma) \right\}, \tag{72}$$

with the kernel given by

$$\tilde{M}(\tau) = \frac{1}{\hbar\beta}\sum_n e^{i\nu_n\tau}\left(\frac{1}{1+\sum_j d_j^2 \dfrac{\nu_n^2}{\nu_n^2+\omega_j^2}} - 1 \right) = -\frac{1}{\hbar\beta}\sum_n e^{i\nu_n\tau}\frac{\sum_j d_j^2 \dfrac{\nu_n^2}{\nu_n^2+\omega_j^2}}{1+\sum_j d_j^2 \dfrac{\nu_n^2}{\nu_n^2+\omega_j^2}} = -\frac{1}{\hbar\beta}\sum_n m_n e^{i\nu_n\tau}. \tag{73}$$

For high temperatures when $\nu_n \to \infty$ one has $\tilde{M}(\tau) =: \delta(\tau): M\Sigma_j d_j^2$ with $M = 1/(1+\Sigma_j d_j^2)$. Combining the friction term with the bare kinetic term then leads to an effective kinetic term of the form $M\dot{Q}^2/2$ so that friction appears simply as an effective mass. Accordingly, the thermal activation factor $\Gamma \propto \exp[-\beta V(Q_b)]$ is independent of friction since it is determined by the constant path at the barrier top $Q=Q_b$, while dissipation influences the prefactor as specified above. The same is true for lower temperatures above the crossover when quantum fluctuations in the rate prefactor lead to an even stronger increase of the escape rate as shown in the previous section.

Below the crossover temperature the contribution of the bounce orbit Q_B dominates the imaginary part of the partition function and the exponential factor in the rate contains its action $S_B = S[Q_B]$—i.e., $\Gamma \propto \exp(-S_B/\hbar)$. Now, let us consider weak friction. In this case we write for the bounce path $Q_B = Q_0 + \delta Q$, where Q_0 is the bounce path in the absence of dissipation, which obeys $\ddot{Q}_0 - V'(Q_0) = 0$. Upon inserting Q_B into the effective action (72) one finds that to lowest order in the friction one has $S_B = S[Q_0] + \Delta S_0$ with

$$\Delta S_0 = \frac{1}{2}\int_0^{\hbar\beta} d\tau \int_0^{\hbar\beta} d\sigma \dot{Q}_0(\tau)\tilde{M}(\tau-\sigma)\dot{Q}_0(\sigma). \tag{74}$$

This correction can be easily expressed in Fourier space by using $Q_0 = (1/\hbar\beta)\Sigma_n Q_n^{(0)} \exp(i\nu_n\tau)$, where one may choose the phase of the bounce such that $Q_n^{(0)} = Q_{-n}^{(0)} = Q_n^{(0)*}$. This way, we find with $m_n = m_{-n}$ and $\nu_n = -\nu_{-n}$ that

$$\Delta S_0 = -\frac{1}{2\hbar\beta}\sum_n |Q_n^{(0)}|^2 \nu_n^2 m_n. \tag{75}$$

Apparently, $\Delta S_0 < 0$ so that $S_B < S_0$, meaning that the probability for quantum tunneling is exponentially *enhanced* due to momentum friction. Physically, since the effective mass of the combined kinetic terms $\tilde{M}(\tau) + : \delta(\tau)$: has Fourier components that are always smaller than 1, the particle's kinetic energy becomes smaller relative to its potential energy. Thus, for a dynamical orbit like the bounce path the action decreases. In contrast, spatial friction leads always to a rate suppression since effectively it provides an additional contribution to the potential energy. For stronger coupling to the heat bath the bounce orbit can easily be calculated numerically along the lines described in [28].

IV. DISCUSSION

In this paper we analyzed the influence of a harmonic heat bath coupled to a system with potential energy via a bilinear interaction between the system's momentum and the individual momenta of the bath degrees of freedom. For a harmonic oscillator and momentum dissipation we find as also noted qualitatively by Cuccoli *et al.* [11] that the coupling to the bath *increases* the delocalization of the position of the oscillator. The thermal variance *increases* with increasing coupling, exactly the opposite of the behavior found for spatial coupling.

For escape over a barrier, in the high-temperature regime, where thermal activation prevails, momentum friction leads to an increase of the flux across the barrier. At somewhat lower temperatures quantum fluctuations come into play and enhance the flux even more. Above the crossover temperature between tunneling and thermal activation, friction appears only in the prefactor of the rate expression. Below the crossover temperature, where quantum tunneling dominates, it reduces the action of the bounce path and thus exponentially increases the decay rate. In contrast to the case of spatial friction, the crossover temperature increases with increasing friction so that for pure momentum coupling quantum effects would be observable even in the high-temperature domain.

In this paper we considered the case of pure momentum coupling. Any realistic system will be influenced by both momentum *and* spatial coupling. The crucial issue is then to what extent the latter one suppresses the impact of the former one. Specific systems to be studied in the future in this respect include molecular compounds, mesoscopic islands coupled to fluctuating charges, and the transport of charged particles moving under the influence of random magnetic fields [13,14].

ACKNOWLEDGMENTS

We thank Professor Y. Makhnovskii for his comments on the manuscript. We also thank the anonymous referees for their comments and especially for bringing to our attention Refs. [11,16]. This work has been supported by grants from the German Israel Foundation for Basic Research and the Israel Science Foundation. J.A. received support through the Heisenberg Programme of the DFG.

[1] H. Risken, *The Fokker-Planck Equation, Methods of Solution and Applications* (Springer-Verlag, Berlin, 1984).
[2] U. Weiss, *Quantum Dissipative System*, 2nd ed. (World Scientific, Singapore, 1999).
[3] A. O. Caldeira and A. J. Leggett, Ann. Phys. (N.Y.) **149**, 374 (1983).
[4] H. Grabert, P. Schramm, and G.-L. Ingold, Phys. Rep. **168**, 115 (1988).
[5] J. Ankerhold, P. Pechukas, and H. Grabert, Phys. Rev. Lett. **87**, 086802 (2001).
[6] E. Pollak, J. Chem. Phys. **85**, 865 (1986).
[7] E. Pollak, in *Dynamics of Molecules and Chemical Reactions*, edited by J. Zhang and R. E. Wyatt (Marcel Dekker, New York, 1996), p. 617.
[8] E. Pollak, Chem. Phys. Lett. **127**, 178 (1986).
[9] E. Pollak, Phys. Rev. A **33**, 4244 (1986).
[10] H. Grabert and U. Weiss, Phys. Rev. Lett. **53**, 1787 (1984).
[11] A. Cuccoli, A. Fubini, V. Tognetti, and R. Vaia, Phys. Rev. E **64**, 066124 (2001).
[12] Y. A. Makhnovskii and E. Pollak, Phys. Rev. E **73**, 041105 (2006).
[13] E. Fermi, Phys. Rev. **75**, 1169 (1949).
[14] P. A. Sturrock, Phys. Rev. **141**, 186 (1966).
[15] D. C. Cole, Phys. Rev. E **51**, 1663 (1995).
[16] A. J. Leggett, Phys. Rev. B **30**, 1208 (1984).
[17] G. W. Ford, J. T. Lewis, and R. F. O'Connell, Phys. Rev. A **37**, 4419 (1988).
[18] A. M. Levine, M. Shapiro, and E. Pollak, J. Chem. Phys. **88**, 1959 (1988).
[19] H. Grabert, U. Weiss, and P. Talkner, Z. Phys. B: Condens. Matter **55**, 87 (1984).
[20] I. Rips and E. Pollak, Phys. Rev. A **41**, 5366 (1990).
[21] I. S. Gradshteyn and I. M. Rhyzhik, *Tables of Integrals, Series, and Products* (Academic, New York, 1981).
[22] J. C. Keck, Adv. Chem. Phys. **13**, 85 (1967).
[23] P. Pechukas, in *Dynamics of Molecular Collisions B*, edited by W. H. Miller (Plenum Press, New York, 1976).
[24] H. A. Kramers, Physica (Amsterdam) **7**, 284 (1940).
[25] R. F. Grote and J. T. Hynes, J. Chem. Phys. **73**, 2715 (1980).
[26] *Handbook of Mathematical Functions*, edited by M. Abramowitz and I. E. Stegun, Nat. Bur. Stand. Appl. Math. Ser. No. 55 (U. S. GPO, Washington, DC, 1972).
[27] P. G. Wolynes, Phys. Rev. Lett. **47**, 968 (1981).
[28] H. Grabert, P. Olschowski, and U. Weiss, Phys. Rev. B **36**, 1931 (1987).